frontiers | Frontiers in Oncology

TYPE Original Research
PUBLISHED 05 December 2024
DOI 10.3389/fonc.2024.1431082

OPEN ACCESS

EDITED BY
Ruijie Yang,
Peking University Third Hospital, China

REVIEWED BY
Jiayao Sun,
Shanghai Proton and Heavy Ion Center (SPHIC), China
Francesco Cuccia,
ARNAS Ospedali Civico Di Cristina Benfratelli, Italy

*CORRESPONDENCE
Yibao Liu
lyb01@tsinghua.org.cn

RECEIVED 11 May 2024
ACCEPTED 18 November 2024
PUBLISHED 05 December 2024

CITATION
Huang Y, Yang J, Song R, Qin T, Yang M and Liu Y (2024) Treating early-stage centrally-located non-small cell lung cancer with DCAT-SBRT in centers lacking the VMAT technique: a comprehensive study. *Front. Oncol.* 14:1431082. doi: 10.3389/fonc.2024.1431082

Treating early-stage centrally-located non-small cell lung cancer with DCAT-SBRT in centers lacking the VMAT technique: a comprehensive study

Yangyang Huang[1,2], Jun Yang[2], Rui Song[2], Tingting Qin[2], Menglin Yang[2] and Yibao Liu[1]*

[1]School of Nuclear Science and Engineering, East China University of Technology, Nanchang, Jiangxi, China, [2]Department of Radiotherapy, the Second Affiliated Hospital of Zhengzhou University, Zhengzhou, Henan, China

Background: Volumetric-modulated arc therapy (VMAT) may have the highest overall performance for stereotactic body radiotherapy (SBRT) treatment of inoperable early-stage NSCLC. However, in centers lacking the VMAT technique, the dynamic conformal arc therapy (DCAT) technique is potentially the best option for small and rounded NSCLC-SBRT. Therefore, we will comprehensively analyze the advantages of the DCAT versus the other techniques except VMAT in terms of dosimetry, plan complexity, delivery time, γ-passing rates and the interplay effect.

Methods: 36 patients with early-stage centrally located NSCLC with PTV volumes < 65 cc were enrolled. All patients were redesigned with 50Gy/5f, and 100% of the prescribed dose was normalized to cover 95% of the PTV. The other two delivery techniques compared to the DCAT technique include 3-dimensional conformal radiotherapy (3DCRT) and intensity-modulated radiotherapy (IMRT), which use the same parameters for all three techniques.

Results: The dosimetric parameters of the 3-group plans all met the RTOG 0813 protocol. Unsurprisingly, plan complexity parameters such as segments and MUs were significantly reduced in the DCAT plans by 159.56 and 925.90 compared to the IMRT plans, respectively (all $P < 0.001$). The delivery time of the DCAT plans was the least of 164.51 s (all $P < 0.05$). Compared to the IMRT plans, the γ-passing rates were higher in the DCAT plans ($P < 0.001$), with the most significant difference of 6.01% in the (2%, 1 mm) criteria. As for the interplay effect, the mean dose difference (MDD) in the DCAT plans was as good as the 3DCRT plans at different respiratory amplitudes but better than the IMRT plans (all $P < 0.05$), and the MDD of DCAT plans did not exceed 3% in all respiratory amplitude.

Conclusion: In centers lacking the VMAT technique, implementing SBRT treatment based on the DCAT technique for inoperable early-stage centrally-located NSCLC patients with PTV volumes < 65 cc achieves better treatment efficiency and delivery accuracy while maintaining the plan quality.

KEYWORDS

DCAT, SBRT, inoperable early-stage centrally-located NSCLC, dosimetric parameter, plan complexity, delivery time, γ-passing rate, interplay effect

1 Introduction

In recent years, the incidence of inoperable early-stage centrally-located non-small cell lung cancer (NSCLC) has been increasing with the increase in population aging and the availability of screening tools (1–3), and the stereotactic body radiotherapy (SBRT) is gradually becoming a standard of care (4–7). The characteristics of SBRT include fewer fractions, higher single doses, higher conformity, and accurate delivery (8). The tumors of early-stage centrally-located NSCLC are close to some critical organs, such as the ipsilateral proximal bronchus tree (PBT) and the healthy lungs, which may be damaged by the high dose of SBRT, thus failing to achieve optimal treatment. Therefore, SBRT planning for inoperable early-stage centrally-located NSCLC requires the most suitable delivery technique (4).

The most common delivery techniques for linac-based SBRT treatment include three-dimension conformal radiotherapy (3DCRT), intensity-modulated radiotherapy (IMRT), dynamic conformal arc therapy (DCAT), and volumetric-modulated arc therapy (VMAT) (9, 10). Many reports have confirmed that the VMAT technique has the highest comprehensive advantage. For example, Dwivedi et al. (11) found that VMAT-based SBRT plans for lung cancer were of better quality, with treatment time decreasing by 57.09% to 60.39% compared to 3DCRT. Xhaferllari et al. (12) concluded that VMAT had a dosimetric advantage compared to fixed-beam IMRT in SBRT treatment of early-stage NSCLC and significantly reduced treatment time. Rauschenbach et al. (13) thought that VMAT could lower the doses of all the organs at risk (OARs) compared to DCAT and 3DCRT. However, in the vast central and western regions of China, many condition-limited centers have only just completed the popularization of the fundamental three-dimension technique and lack the hardware and software to implement the VMAT technique, and the available SBRT techniques are 3DCRT, IMRT, and DCAT.

The 3DCRT technique has the most straightforward plan complexity of these three techniques and lacks the intensity modulation capability to protect adjacent OARs. In contrast, the IMRT technique is superior to the 3DCRT technique in almost all dosimetric parameters (14, 15). The DCAT technique is traditionally just the arc 3DCRT technique, which is not much different from the 3DCRT technique in OAR-sparing (16). However, the novel DCAT technique based on the Monaco treatment planning system (TPS) incorporates two new improvements, namely, variable dose rate (VDR) and segment shape optimization (SSO), which allow the linac to reduce the dose rate where a limited dose is needed, and allow the multi-leaf collimator (MLC) to move within a 5-mm range in and out of the targets, thus effectively improving the plan quality (17, 18). As a result, excellent dosimetric quality of the DCAT technique is demonstrated in treating small, rounded targets. Rauschenbach et al. (13) concluded that the DCAT technique was superior in high and low-dose spillage compared to the 3DCRT technique in the NSCLC-SBRT. Ming et al. (19) found that the mean heart dose of DCAT and IMRT were 2.3 Gy and 5.2 Gy in lung cancer radiotherapy, respectively, meaning that the DCAT technique was better than the IMRT in heart-sparing. Shi et al. (20) thought the DCAT technique was valuable and efficient for lung SBRT planning, and the plan quality met the RTOG protocols.

Several reports showed that the DCAT technique had advantages regarding plan complexity, delivery time and the γ-passing rates. Ong et al. (21) found that the MU efficiency (MU/Gy) was 187 ± 20, 179 ± 18, and 445 ± 84 for DCAT, 3DCRT and IMRT plans. Rauschenbach et al. (13) thought that when the single dose was normalized to deliver 20 Gy for comparison purposes, the mean MUs were 1880 ± 1260, 2540 ± 2020, and 3580 ± 1900, respectively, for DCAT, 3DCRT and VMAT. Moon et al. (22) concluded that the delivery time in liver SBRT for DCAT and VMAT were 3.6 ± 0.5 min and 4.5 ± 0.7 min, respectively. Lee et al. (23) considered that the γ-passing rate in lung SBRT for DCAT was 97.60 ± 2.41% under 2%/2mm criteria, which was high enough for accurate delivery.

An influencing factor that cannot be neglected during dose delivery in early-stage centrally-located NSCLC is respiratory motion, which may lead to deviations between the planned and delivered dose distributions in the form of dose blurring and interplay effects (24). Regardless of whether 3DCRT, IMRT or DCAT technique is used, dose blurring occurs, resulting in hot spots and cold spots in the target volume and an increasing dose to the adjacent OARs, so every effort must be made to minimize the interplay effects. Of these three techniques, the DCAT is less vulnerable to interplay effects. Netherton et al. (25) thought that the simpler the IMRT plan complexity, the lower the interplay effect. Burton et al. (26) found that the DCAT plans were sufficiently robust to overcome the interplay effect, which meant that the DCAT plans had a mean value of 6%

dose deviation. However, the VMAT plans had a mean value of up to 21% dose deviation in single-fraction lung SBRT utilizing flattening filter-free (FFF) beams. Seco et al. (27) thought that daily intrafraction dose variation of more than 10% in IMRT plans was non-negligible and could potentially lead to biological effects.

Most of the literature has focused on only the dosimetric advantage of the DCAT technique, with few comprehensive analyses of its dosimetry, plan complexity, delivery time, the γ-passing rates and the interplay effect. This paper will comprehensively analyze the above factors to provide a reference for implementing SBRT using the DCAT technique in inoperable early-stage centrally-located NSCLC.

2 Methods

2.1 Patient cohort

Thirty-six consecutive patients with inoperable early-stage centrally-located NSCLC treated with SBRT were retrospectively selected after obtaining approval from the Ethics Committee of the Second Affiliated Hospital of Zhengzhou University (ethics number: 2023202). Due to its retrospective design, the Ethics Committee of the Second Affiliated Hospital of Zhengzhou University waived the need to obtain informed patient consent. All methods were carried out following relevant guidelines and regulations. The general conditions of the patients are shown in Table 1. Based on the RTOG 0236 and 0813 protocols (28, 29), the screened patients were required to fulfill the following criteria: planning target volume (PTV) no larger than 5 cm and located outside the 0.5 cm area and within the 2 cm area of the ipsilateral PBT or immediately adjacent to the mediastinal or pericardial pleura. Exclusion of patients with the tumors' extent cannot be defined on CT (e.g., solid lesions around the tumor or lung atelectasis) and patients with ultracentral lung tumors.

2.2 Positioning and contouring

Scanning was performed with 4DCT. Each patient underwent scanning on a 16-row big-bore CT scanner (Philips Medical Systems, Cleveland, OH) with a slice thickness of 3 mm.

TABLE 1 Summary of patients' general conditions.

Item	Descriptions
Tumor Stage	14 cases of T1N0M0, 22 cases of T2N0M0
Age	32 to 73 years old, median age 51
Gender	19 males and 17 females
Tumor Location	13 cases in the lower lobe of the left lung, 14 cases in the lower lobe of the right lung and 9 cases in the middle lobe of the right lung
Target Size	ITV volume between 2.01 – 23.15 cc, average 16.64 cc; PTV volume between 5.82 – 63.78 cc, average 29.49 cc, max < 65 cc

ITV, internal target volume; PTV, planning target volume.

All patients were placed in the supine position, with their arms holding a handle above their heads. The thoracic area was fixed using a thermoplastic film (Guangzhou Klarity Medical Equipment Co., Ltd., Guangzhou, China). The scanning range included all OARs to be evaluated. The recommended range was from the upper edge of the cricoid cartilage to the upper edge of the vertebral body of lumbar 2, with a minimum of 10 cm above the upper and lower boundaries of the tumors. The internal target volume (ITV) was delineated on the maximum intensity projection CT (MIPCT) by a radiation oncologist with expertise in lung SBRT. Based on the 4DCT, all patients had a respiratory amplitude of ≤ 5 mm in the 3D direction during free breathing. The PTV was created by adding an isotropic 5 mm margin to the ITV according to the RTOG recommendations (28, 30). The average intensity projection CT (AIPCT) was used for planning and dose calculations.

The OARs to be delineated included the ipsilateral lung and lung all (both excluding the ITV, total named as healthy lungs), the ipsilateral PBT, the spinal cord, the esophagus, the great vessels, the heart, the ipsilateral brachial plexus, and the skin.

2.3 Planning

The 3-group plans were redesigned for each patient in Monaco TPS (V6.0, Elekta Solution AB, Kungstensgatan 18, Stockholm, Sweden) using the XVMC (X-ray Voxelized Monte Carlo) algorithm (17). All the plans were delivered by an Infinity Linac equipped with an Agility collimator and a 6 MV X-ray beam (1400 MU/min). The prescription for all plans was 50 Gy/5 f.

In the 3DCRT plans, ten static, noncoplanar and nonopposing beams were used, and eight on the ipsilateral side at 30° intervals (table angle 0°) and two on the anterior side (table angle 90°), with the isocenter placed at the center of the PTV. Beam directions and weights were manually optimized according to the tumor location, mainly to achieve the mediastinal OAR-sparing. All beams in the 3DCRT plans used a collimation angle of 0°. The geometry for the IMRT plans was the same as for the 3DCRT plans. The IMRT delivery method was dynamic MLC, and the segment sequencing options were chosen as SSO and High Precision Leaf Position. The maximum number of segments per beam was 30, the minimum segment width was 0.70 cm, and the fluence smoothing option was medium and max. Sweep Efficiency and Allow Move Only Segments were selected. In the DCAT plans, two 210° arcs (table angle 0°) on the ipsilateral side, plus a 60° anterior arc (table angle 90°) were used, with the isocenter placed at the center of the PTV. The DCAT plans used different collimation angles between ±45° for each arc to minimize the tongue-and-groove effect (31). The angular increment was set to 10°, and SSO and VDR were selected. All plans' dose grid and statistical uncertainty were 2.0 mm and 1%, respectively, and the Target Margin was selected as 0-1 mm.

In IMRT and DCAT planning, the dose constraints of the ipsilateral lung and the ipsilateral PBT should be met first and even prioritized over the PTV dose coverage. All plans were rescaled to fulfill 95% of the PTV covered by 100% prescription dose, and > 99% of the ITV covered by 100% prescription dose, and all hot spots

(between 120% and 150% prescription dose) were located within the ITV. If mediastinal OARs overlap the PTV, the minimum dose for the PTV and ITV should be at least 70% and 90% of the prescription dose, respectively.

2.4 Dosimetric evaluation

The PTV was evaluated using $D_{98\%}$, $D_{2\%}$, homogeneity index (HI), conformity index (CI), and $R_{50\%}$, respectively, where $D_{98\%}$ and $D_{2\%}$ represent the PTV's approximate minimum and maximum dose. Based on the RTOG 0813 protocol, $D_{2\%}$ decreases with decreasing PTV. At PTV = 70 cc, $D_{2\%}$ was < 86.0 Gy; at PTV = 50 cc, $D_{2\%}$ was <77.0 Gy; and at PTV < 10 cc, $D_{2\%}$ was < 57.0 Gy. For all PTV, $D_{98\%}$ was > 45.0 Gy. CI (32) and $R_{50\%}$ were used to describe the high and intermediate dose spillage for the 3-group plans. CI=PIV/TV, where PIV is the prescription isodose volume, and TV is the target volume. The value of CI is ≥1, where the closer the CI is to 1, the better. According to the RTOG 0813 protocol, CI < 1.5, preferably < 1.2. $R_{50\%}$ represents the 50% prescription isodose volume ratio to the PTV. Based on the RTOG 0813 protocol, $R_{50\%}$ increases as the PTV decreases. For example, $R_{50\%}$ is < 4.8 at PTV = 70 cc, $R_{50\%}$ is < 5.0 at PTV = 50 cc, and $R_{50\%}$ is < 7.5 at PTV <10 cc. HI describes the dose homogeneity degree within the PTV, HI = $D_{5\%}/D_{95\%}$ (33), where $D_{5\%}$ and $D_{95\%}$ represent the dose to cover 5% and 95% of the PTV, respectively. A lower HI is preferred, but pursuing a homogeneous dose within the PTV increases the OAR dose. Therefore, when the PTV does not contain organs that need to be preserved (34), the maximum HI should be set with caution. Based on the clinical practice in the department, HI < 1.6 is generally considered appropriate.

OARs were compared in compliance with the RTOG 0813 protocol and other relevant requirements in the literature (35, 36), including ipsilateral lung V_{5Gy} < 60% and V_{20Gy} < 20%, lung all V_{5Gy} < 40% and V_{20Gy} < 10%; ipsilateral PBT V_{18Gy} < 4 cc and D_{max} < 52.5 Gy; spinal cord $V_{22.5Gy}$ < 0.25 cc, $V_{13.5Gy}$ < 0.5 cc and D_{max}< 32 Gy; esophagus $V_{27.5Gy}$ < 5 cc and D_{max} < 52.5 Gy; heart V_{32Gy} < 15 cc and D_{max} < 52.5 Gy; great vessels V_{47Gy} < 10 cc and D_{max} < 52.5 Gy; ipsilateral brachial plexus V_{30Gy} < 3 cc and D_{max} < 32 Gy; skin V_{30Gy} < 10 cc and D_{max} < 32 Gy.

2.5 Plan complexity, delivery time, and the γ-passing rates

Plan complexity was weighted based on segments and MUs, as segments and MUs positively correlate with plan complexity (37). Delivery time was related to delivery efficiency, and they were recorded when measuring γ-passing rates using SRS MapCHECK (equipped with the StereoPHAN phantom) (Sun Nuclear, Melbourne, FL). Based on the AAPM TG-218 report and other documentation (38, 39), and taking into account the clinical practice in the department, the γ-passing rates were 2%/2mm > 95%, 2%/1mm > 85%, and 1%/2mm > 90%, while excluding data below 10% of the maximum dose.

2.6 Interplay effect

The interplay effects of the 3-group plans were all performed on a programmable dynamic respiratory phantom (CIRS 008A, Computer Imaging Reference Systems, Norfolk, USA). This phantom consists of a static chest model and a moving lung-equivalent rod with a spherical water-equivalent target that simulates a tumor's motion. The study simulated the respiratory movements through a one-dimensional motion in the cranial-caudal direction.

A representative respiratory motion function was used to simulate the respiratory motion profile (40, 41). The motion function is defined as,

$$A = A_0 \sin^6(\pi t/T) \quad (1)$$

where t is the time, A_0 is the respiratory amplitude, and T is the respiratory period. The respiratory movements of three respiratory amplitudes (20, 10 and 5 mm, peak-to-peak) were simulated for a 5 s respiratory period.

The point dose at the center of the target volume (phantom center) was measured using a center-located microdiamond detector (PTW, Freiburg, Germany) with a minimum sensitive volume of 0.004 mm^3, as shown in Figure 1. The detector was cross-calibrated in water against a 0.6 cc farmer type chamber calibrated in a primary laboratory. Considering that the cable of the microdiamond detector is likely to generate artifacts on the CT of the phantom, and other tool will be used to measure the γ-passing rates of the plans, the phantom was used to directly measure the static point doses, and then measured the dynamic point doses under different respiratory amplitudes respectively. Starting from a random respiration phase, each of the collection was repeated three times per respiration amplitude for averaging, and the absolute value of the difference between the measured dynamic and static dose divided by the static dose was used to quantify the interplay effect, named as mean dose difference (MDD).

2.7 Statistical analysis

Data were analyzed using SPSS 25.0 (IBM SPSS Statistics for Windows, IBM Corp Version 25.0. Armonk, NY). The paired non-parametric Wilcoxon signed-rank test was used to compare any two plans. The confidence interval was 95%, with $P < 0.05$ indicating a statistically significant difference.

3 Results

3.1 Dosimetric parameters

As can be seen in Table 2, the 3-group plans all met the RTOG 0813 protocol. The $D_{2\%}$, $D_{98\%}$, and HI of the 3-group plans were very similar, and the differences were not statistically significant (all $P > 0.05$). Figures 2, 3 show the transverse and coronal isodose lines and the DVH for the same case of the 3-group plans, and it can be

10.3389/fonc.2024.1431082

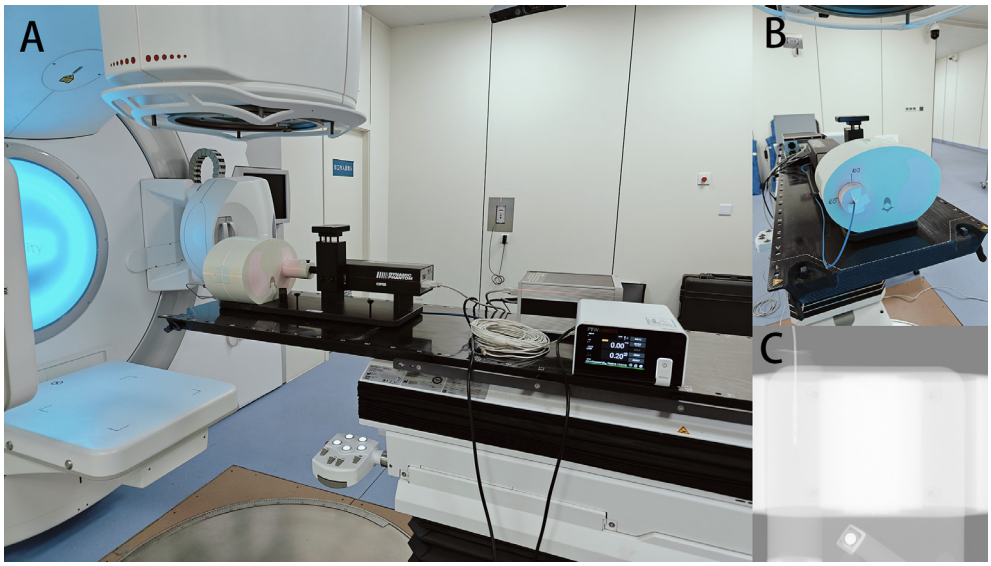

FIGURE 1
Schematic diagram of the combined use of the CIRS 008A phantom and the PTW microdiamond detector. **(A)** lateral view; **(B)** front view; **(C)** X-ray fluoroscopic view.

TABLE 2 Summary of dosimetric parameters for the 3-group plans.

Parameters (mean [SD])		3DCRT (A)	IMRT (B)	DCAT (C)	*P* value		
					A VS. B	A VS. C	B VS. C
PTV	$D_{98\%}$(Gy)	44.86 (1.23)	43.59 (1.81)	44.02 (2.84)	0.953	0.886	0.518
	$D_{2\%}$(Gy)	61.80 (2.87)	66.69 (3.11)	64.55 (5.62)	0.051	0.083	0.178
	HI	1.29 (0.05)	1.27 (0.05)	1.28 (0.10)	0.127	0.072	0.913
	CI	1.36 (0.11)	1.11 (0.04)	1.15 (0.04)	0.008*	0.011*	0.005*
	$R_{50\%}$	5.64 (0.74)	4.36 (0.53)	5.01 (0.62)	<0.001*	0.015*	0.001*
Ipsilateral PBT	V_{18Gy} (%)	3.15 (1.12)	3.23 (1.12)	3.04 (1.06)	0.374	0.445	0.291
	D_{max} (Gy)	51.40 (2.99)	50.25 (3.41)	46.10 (3.74)	0.674	<0.001*	<0.001*
Ipsilateral lung	V_{5Gy} (%)	36.36 (7.33)	37.01 (7.00)	39.44 (7.99)	0.008*	<0.001*	<0.001*
	V_{20Gy} (%)	10.75 (3.43)	7.65 (2.68)	9.53 (3.61)	<0.001*	0.066	<0.001*
Lung all	V_{5Gy} (%)	18.60 (4.52)	20.55 (6.09)	21.71 (6.71)	0.006*	<0.001*	<0.001*
	V_{20Gy} (%)	5.80 (1.43)	3.71 (0.27)	4.59 (1.88)	<0.001*	0.005*	<0.001*
Spinal cord	D_{max} (Gy)	11.95 (2.57)	9.74 (2.70)	10.11 (5.36)	0.048*	0.260	0.648
Esophagus	D_{max} (Gy)	21.37 (6.98)	20.70 (10.66)	20.55 (11.63)	0.173	0.069	0.850
Heart	V_{32Gy} (%)	2.50 (3.16)	1.31 (2.04)	1.12 (1.85)	0.028*	<0.001*	0.465
	D_{max} (Gy)	39.55 (13.39)	35.97 (15.76)	34.45 (15.20)	<0.001*	0.008*	0.018*
Great vessels	V_{47Gy} (%)	0.20 (0.28)	0.09 (0.18)	0.16 (0.39)	0.310	0.635	0.199
	D_{max} (Gy)	48.52 (4.82)	42.51 (9.93)	40.57 (10.87)	0.263	0.031*	0.118
Ipsilateral brachial plexus	D_{max} (Gy)	0.33 (0.30)	0.32 (0.15)	0.28 (0.25)	0.377	0.112	0.385
Skin	D_{max} (Gy)	10.53 (1.04)	14.60 (1.15)	9.74 (1.99)	0.008*	0.224	<0.001*

SD, standard deviation; 3DCRT, 3-dimensional conformal radiotherapy; IMRT, intensity-modulated radiotherapy; DCAT, dynamic conformal arc therapy; VS., versus; PTV, planning target volume; $D_{98\%}$, dose to 98% of the target volume; $D_{2\%}$, dose to 2% of the target volume; HI, homogeneity index; CI, conformity index; $R_{50\%}$, the ratio of the 50% prescription isodose volume to the PTV; PBT, proximal bronchial tree; $V_{x\ Gy}$, the ratio of the volume received > x Gy dose by an organ to the total volume; D_{max}, the maximum point dose to an organ. A statistically significant difference result is indicated by an asterisk (*).

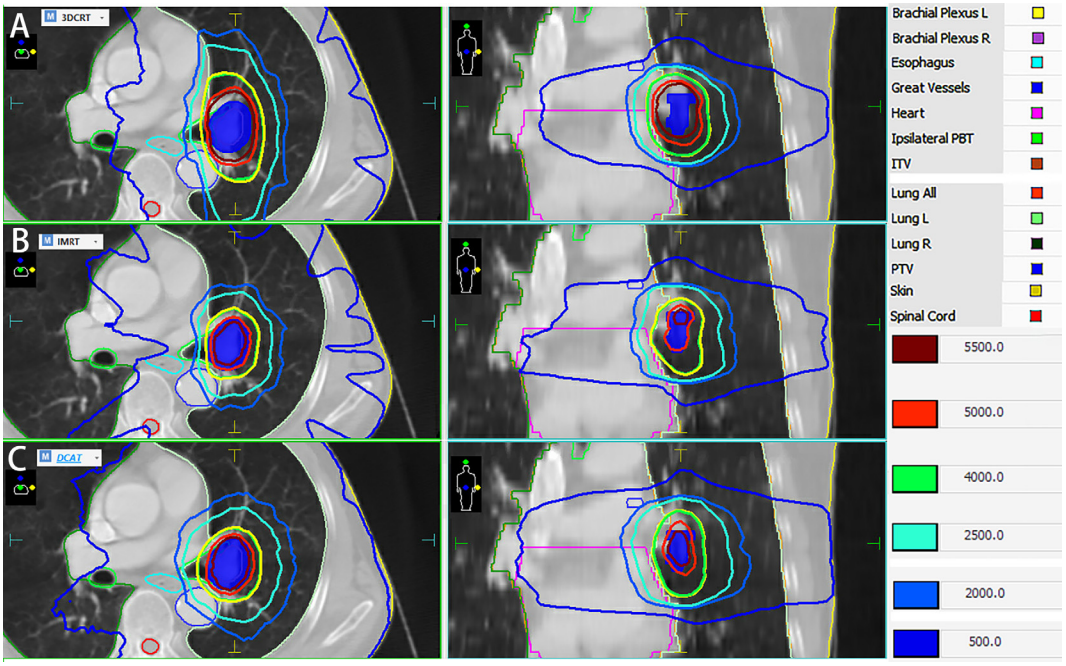

FIGURE 2
Dose distribution of the same case of 3DCRT (Group **A**), IMRT (Group **B**) and DCAT plans (Group **C**). The DCAT plan has a relatively uniform target dose distribution than the IMRT plan, and a tighter dose distribution than the 3DCRT plan.

seen that the DCAT plan had a more uniform target dose than the IMRT plan and a better OAR-sparing than the 3DCRT plan. The mean CI value of the DCAT plans was between IMRT plans and 3DCRT plans, and the differences were statistically significant (all $P < 0.05$). The mean $R_{50\%}$ of the DCAT plans was not as good as that of the IMRT plans but better than the 3DCRT plans, with a mean value of 5.01, and the differences were statistically significant (all $P < 0.05$).

The DCAT plans were superior in the ipsilateral PBT-sparing among the 3-group plans, especially in the D_{max} parameter (all $P < 0.001$). The evaluation parameters of the healthy lungs in the DCAT plans were all inferior to those in the IMRT plans but were superior to those in the 3DCRT plans (Lung All V_{20Gy}). However, the most significant difference in mean value among the 3-group plans was only 7.81% higher (DCAT vs. 3DCRT, ipsilateral lung V_{5Gy}). For the remaining OARs listed in Table 2, the corresponding

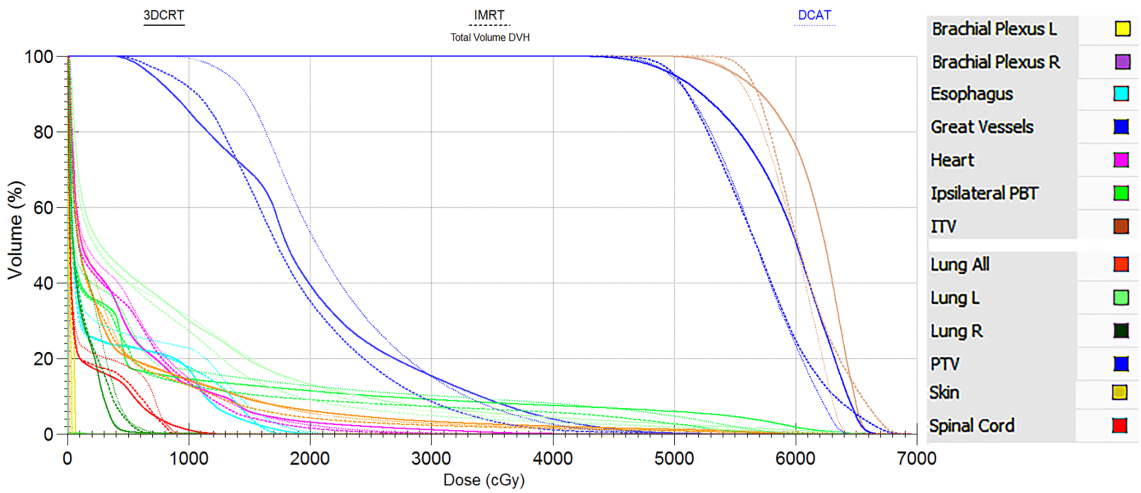

FIGURE 3
DVH comparison of the same case between 3DCRT (solid line), IMRT (long dash line) and DCAT plans (short dash line). The legend is displayed in the right side. DVH similarly supports the view that the DCAT plan has a relatively uniform target dose distribution than the IMRT plan, and a better OAR-sparing than the 3DCRT plan.

parameters of the DCAT plans were mostly between 3DCRT and IMRT plans, and the 3-group plans were all above the qualified line. Some of the OARs' data were not presented in Table 2 because all the values among the 3-group plans were 0 (spinal cord $V_{22.5Gy}$, ipsilateral brachial plexus V_{30Gy}, and skin V_{30Gy}), or the majority of them were 0 (spinal cord $V_{13.5Gy}$, esophagus $V_{27.5Gy}$).

3.2 Plan complexity, delivery time, the γ-passing rates, and the interplay effect

Regarding the plan complexity, the DCAT plans showed a significant reduction in segments and MUs compared to the IMRT plans, mean reduction in segments by 159.56 and MUs by 925.90 *(all* $P < 0.001$), as shown in Table 3. The mean delivery time of the DCAT plans was the least of 164.51 s (all $P < 0.05$). The γ-passing rates of 3-group plans were qualified under different criteria (2%/2mm, 1%/2mm, and 2%/1mm), as shown in Table 3. However, the γ-passing rates of the DCAT plans were higher than those of the IMRT plans under all criteria ($P < 0.001$), and the advantage became more and more evident as the criteria became more and more stringent. For example, under the criteria of (2%/1mm), the γ-passing rates of the DCAT plans got a mean improvement of 6.01% compared to the IMRT plans ($P < 0.001$). As for the interplay effect, with the respiratory amplitude decreased, the MDD decreased in all the 3-group plans. At different respiratory amplitudes, the MDD in the DCAT plans was as good as the 3DCRT plans but better than the IMRT plans (all $P < 0.05$). The MDD of DCAT plans did not exceed 3% at expected respiratory amplitudes.

4 Discussion

In this paper, we compared the dosimetric parameters, plan complexity, delivery time, the γ-passing rates, and the interplay effect of the 3DCRT, the DCAT, and the IMRT plans for 36 patients with inoperable early-stage centrally-located NSCLC (PTV < 65 cc), and analyzed the feasibility of the DCAT plans to implement SBRT treatment (50Gy/5fx). The results showed that all dosimetric parameters of the 3-group plans met the RTOG 0813 protocol, and the DCAT plans showed the highest comprehensive advantage.

As shown in Table 2 and Figure 2, the $D_{2\%}$, $D_{98\%}$, and HI of the DCAT plans were very similar to the other two plans (all $P > 0.05$), and the DCAT plans had moderate CI and $R_{50\%}$ values among the 3-group plans. The above results are similar to the findings of several authors. For example, Goto et al. (16) found that the DCAT plans (median 1.3) had better CI than the 3DCRT plans (median 2.2), which was similar to the results of Peterlin et al. (42). Yau et al. (43) thought that the DCAT plans could offer similar dosimetric benefit compared to the IMRT plans. It is reported that the clinical outcomes of the DCAT plans were pretty good, and the 1-year local control of DCAT-SBRT was 96.7%, 1-year overall survival was 93.1% in early-stage lung cancer (44).

The most common side effects of SBRT treatment for centrally-located lung cancer include fatal hemoptysis (45) and fatal radiation pneumonitis in patients with poor respiratory function (46–48), particularly those with underlying interstitial lung disease. Therefore, the dose to the ipsilateral PBT and healthy lungs must be strictly controlled according to the RTOG 0813 protocol. As shown in Table 2, the DCAT plans were superior in protecting the ipsilateral PBT in parameters of D_{max} (all $P < 0.001$). The lung evaluation parameters in the 3-group plans were substantially lower than the RTOG 0813 protocol, and the DCAT plans got relatively lower V_{20Gy}. It has been reported that only 4.6% of symptomatic grade 2 radiation pneumonitis in similar lung evaluation parameters in the DCAT plans (44). In addition, Table 2 showed the DCAT plans had advantages in most remain OARs. In summary, all three techniques produced dosimetrically qualified plans much smaller in absolute values than those required by the RTOG0813 protocol. Therefore, no significant differences in radiotoxicity were expected.

TABLE 3 Summary of other parameters for the 3-group plans.

Parameters (mean [SD])		3DCRT (A)	IMRT (B)	DCAT (C)	*P* value		
					A VS. B	A VS. C	B VS. C
Segments	N/A	10	261.68 (11.10)	102.12 (27.25)	N/A	N/A	<0.001*
MUs	N/A	1648.93 (76.43)	2781.36 (451.68)	1855.46 (269.34)	0.008*	0.842	<0.001*
Delivery time (s)	N/A	192.32 (18.54)	253.47 (23.97)	164.51 (15.07)	<0.001*	0.017*	<0.001*
γ-passing rates (%)	(2%/2mm)	99.27 (0.45)	96.34 (1.98)	98.99(1.11)	<0.001*	0.674	<0.001*
	(1%/2mm)	97.16 (1.87)	93.61 (2.78)	96.85(1.97)	<0.001*	0.138	<0.001*
	(2%/1mm)	93.55 (2.98)	87.13 (3.77)	93.14 (2.91)	<0.001*	0.164	<0.001*
MDD (%)	20mm	2.05 (1.62)	4.39 (5.47)	2.84 (2.48)	<0.001*	0.321	0.035*
	10mm	1.68 (0.56)	3.73 (4.68)	1.89 (1.45)	<0.001*	0.647	0.006*
	5mm	0.78 (0.22)	2.35 (1.49)	1.08 (0.14)	<0.001*	0.257	0.014*

SD, standard deviation; 3DCRT, 3-dimensional conformal radiotherapy; IMRT, intensity-modulated radiotherapy; DCAT, dynamic conformal arc therapy; VS., versus; MUs, monitor units; N/A, not applicable; MDD, mean dose difference. A statistically significant difference result is indicated by an asterisk (*).

In addition to the dosimetric advantage, the most significant advantages of the DCAT plans are suitable plan complexity, delivery time, γ-passing rates, and the interplay effect (49–52). As can be seen in Table 3, the DCAT plans required fewer segments and MUs to deliver the same dose compared to the IMRT plans (13), with an average reduction in segments and MUs of 159.56 and 925.90, respectively (all $P < 0.001$). As a result, the mean delivery time of the DCAT plans was the least of 164.51 s (all $P < 0.05$), which could improve the patient's comfort, especially in deep inspiration breath-hold radiotherapy (53). Another benefit of fewer segments and MUs may be the higher γ-passing rates compared to the IMRT plans (54). The results in Table 3 showed that the γ-passing rates in the DCAT plans were more significant than that in the IMRT plans under all criteria ($P < 0.001$), and the advantage became more and more evident as the criteria became more and more stringent. This is due to the rounded segment shape and large segment area of the DCAT plans (17, 18, 44, 53, 55). Table 3 also showed that the DCAT plans had a relatively lower interplay effect among the 3-group plans. At expected respiratory amplitudes (5-20 mm), the MDD did not exceed 3%. The interplay effect can lead to hot and cold spots within the target (40), reducing the tumor control probability. The study showed that the interplay effect of the DCAT plans was significantly smaller than that of the IMRT plans but similar to the 3DCRT plans. Considering the MLC leaves in the DCAT plans moved around the edge of the moving target, the findings of this study were consistent with the study of Ge et al. (50). This is especially critical in the SBRT treatment of NSCLC with respiratory motion. After all, the interplay effect is one of the biggest concerns in conducting chest SBRT treatment in the free-breathing condition (56). Therefore, the DCAT technique may be the best choice in some condition-limited centers when implementing inoperable early-stage centrally-located NSCLC SBRT (57).

Implementing the DCAT plans in this paper is based on two premises. The first point is that the targets must be far from the OARs (58), especially the ipsilateral PBT because the DCAT plans have low dose modulation and are less capable of OAR-sparing. The second point is that the maximum PTV volume included in this paper is < 65 cc, so no analysis is given for a larger PTV volume. One of the shortcomings of this paper is that it does not involve the research on multiple lesions. Therefore, we look forward to conducting in-depth research on radiotherapy techniques for multiple lesions in the upcoming experiments.

5 Conclusions

In centers lacking the VMAT technique, the study herein supports the DCAT technique as the first choice for SBRT treatment of inoperable early-stage centrally-located NSCLC (PTV < 65cc) because of certain advantages in terms of adequate OAR-sparing, less treatment time, high γ-passing rates, and low interplay effect.

Data availability statement

The original contributions presented in the study are included in the article/supplementary material. Further inquiries can be directed to the corresponding author.

Ethics statement

The studies involving humans were approved by The Ethics Committee of the Second Affiliated Hospital of Zhengzhou University. The studies were conducted in accordance with the local legislation and institutional requirements. Written informed consent for participation was not required from the participants or the participants' legal guardians/next of kin in accordance with the national legislation and institutional requirements.

Author contributions

YH: Data curation, Formal analysis, Investigation, Software, Visualization, Writing – original draft, Writing – review & editing. JY: Supervision, Validation, Visualization, Writing – review & editing. RS: Supervision, Writing – review & editing. TQ: Investigation, Software, Writing – original draft, Writing – review & editing. MY: Methodology, Software, Writing – original draft, Writing – review & editing. YL: Conceptualization, Funding acquisition, Project administration, Resources, Validation, Writing – original draft, Writing – review & editing.

Funding

The author(s) declare financial support was received for the research, authorship, and/or publication of this article. Research reported in this publication was supported by the Henan Science and Technology under award number 232102310091, Henan Medical Science and Technology Foundation under award number LHGJ20210407, and National Natural Science Foundation of China under award number 11965001.

Conflict of interest

The authors declare that the research was conducted in the absence of any commercial or financial relationships that could be construed as a potential conflict of interest.

Publisher's note

References

1. Guckenberger M, Andratschke N, Alheit H, Holy R, Moustakis C, Nestle U, et al. Definition of stereotactic body radiotherapy: principles and practice for the treatment of stage I non-small cell lung cancer. *Strahlenther Onkol*. (2014) 190:26–33. doi: 10.1007/s00066-013-0450-y

2. Haasbeek CJA, Palma D, Visser O, Lagerwaard FJ, Slotman B, Senan S. Early-stage lung cancer in elderly patients: a population-based study of changes in treatment patterns and survival in the Netherlands. *Ann Oncol*. (2012) 23:2743–47. doi: 10.1093/annonc/mds081

3. Chang JY, Senan S, Paul MA, Mehran RJ, Louie AV, Balter P, et al. Stereotactic ablative radiotherapy versus lobectomy for operable stage I non-small-cell lung cancer: a pooled analysis of two randomised trials. *Lancet Oncol*. (2015) 16:630–7. doi: 10.1016/s1470-2045(15)70168-3

4. Bang A, Bezjak A. Stereotactic body radiotherapy for centrally located stage I non-small cell lung cancer. *Transl Lung Cancer Res*. (2019) 8:58–69. doi: 10.21037/tlcr.2018.10.07

5. Kepka L, Socha J. Dose and fractionation schedules in radiotherapy for non-small cell lung cancer. *Transl Lung Cancer Res*. (2021) 10:1969–82. doi: 10.21037/tlcr-20-253

6. Chang JY, Bezjak A, Mornex F. Stereotactic ablative radiotherapy for centrally located early stage non-small-cell lung cancer: what we have learned. *J Thorac Oncol*. (2015) 10:577–85. doi: 10.1097/jto.0000000000000453

7. Davis JN, Medbery C, Sharma S, Pablo J, Kimsey F, Perry D, et al. Stereotactic body radiotherapy for centrally located early-stage non-small cell lung cancer or lung metastases from the RSSearch(®) patient registry. *Radiat Oncol*. (2015) 10:113. doi: 10.1186/s13014-015-0417-5

8. Videtic GMM, Donington J, Giuliani M, Heinzerling J, Karas TZ, Kelsey CR, et al. Stereotactic body radiation therapy for early-stage non-small cell lung cancer: Executive Summary of an ASTRO Evidence-Based Guideline. *Pract Radiat Oncol*. (2017) 7:295–301. doi: 10.1016/j.prro.2017.04.014

9. Badellino S, Muzio JD, Schivazappa G, Guarneri A, Ragona R, Bartoncini S, et al. No differences in radiological changes after 3D conformal vs VMAT-based stereotactic radiotherapy for early stage non-small cell lung cancer. *Br J radiology*. (2017) 90:20170143. doi: 10.1259/bjr.20170143

10. Stathakis S, Narayanasamy G, Licon AL, Myers P, Li Y, Crownover R, et al. A dosimetric comparison between volumetric-modulated arc therapy and dynamic conformal arc therapy in SBRT. *J B.U.ON: Off J Balkan Union Oncol*. (2019) 24:838–43.

11. Dwivedi S, Kansal S, Shukla J, Bharati A, Dangwal VK. Dosimetric evaluation of different planning techniques based on flattening filter-free beams for central and peripheral lung stereotactic body radiotherapy. *Biomed Phys Eng express*. (2021) 77. doi: 10.1088/2057-1976/ac2f0d

12. Xhaferllari I, El-Sherif O, Gaede S. Comprehensive dosimetric planning comparison for early-stage, non-small cell lung cancer with SABR: fixed-beam IMRT versus VMAT versus TomoTherapy. *J Appl Clin Med Phys*. (2016) 17:329–40. doi: 10.1120/jacmp.v17i5.6291

13. Rauschenbach BM, Mackowiak L, Malhotra HK. A dosimetric comparison of three-dimensional conformal radiotherapy, volumetric-modulated arc therapy, and dynamic conformal arc therapy in the treatment of non-small cell lung cancer using stereotactic body radiotherapy. *J Appl Clin Med Phys*. (2014) 15:4898. doi: 10.1120/jacmp.v15i5.4898

14. Merrow CE, Wang IZ, Podgorsak MB. A dosimetric evaluation of VMAT for the treatment of non-small cell lung cancer. *J Appl Clin Med Phys*. (2012) 14:4110. doi: 10.1120/jacmp.v14i1.4110

15. Cai J, Malhotra HK, Orton CG. Point/Counterpoint. A 3D-conformal technique is better than IMRT or VMAT for lung SBRT. *Med Phys*. (2014) 41:040601. doi: 10.1118/1.4856175

16. Goto M, Sanuki N, Kasae M, Terabayashi R, Nishiwaki Y, Ogita Y, et al. Dynamic conformal arc radiotherapy for locally advanced lung cancer: a comparison with static-beam conformal radiotherapy. *Rep Pract Oncol Radiother*. (2022) 27:897–904. doi: 10.5603/RPOR.a2022.0106

17. Clements M, Schupp N, Tattersall M, Brown A, Larson R. Monaco treatment planning system tools and optimization processes. *Med Dosim*. (2018) 43:106–17. doi: 10.1016/j.meddos.2018.02.005

18. Kim S, Kim T, Ko SJ, Serago C, Smith A, Vallow LA, et al. Negative margin technique - a novel planning strategy to improve dose conformation in SBRT using dynamic conformal arc delivery. *J Appl Clin Med Phys*. (2013) 14:79–89. doi: 10.1120/jacmp.v14i5.4283

19. Ming X, Feng Y, Liu H, Zhang Y, Zhou L, Deng J. Cardiac exposure in the dynamic conformal arc therapy, intensity-modulated radiotherapy and volumetric modulated arc therapy of lung cancer. *PloS One*. (2015) 10:e0144211. doi: 10.1371/journal.pone.0144211

20. Shi C, Tazi A, Fang DX, Iannuzzi C. Implementation and evaluation of modified dynamic conformal arc (MDCA) technique for lung SBRT patients following RTOG protocols. *Med Dosim*. (2013) 38:287–90. doi: 10.1016/j.meddos.2013.02.010

21. Ong CL, Verbakel WF, Cuijpers JP, Slotman BJ, Lagerwaard FJ, Senan S. Stereotactic radiotherapy for peripheral lung tumors: a comparison of volumetric modulated arc therapy with 3 other delivery techniques. *Radiother Oncol*. (2010) 97:437–42. doi: 10.1016/j.radonc.2010.09.027

22. Moon YM, Jeon W, Yu T, Bae SI, Kim JY, Kang JK, et al. Which is better for liver SBRT: dosimetric comparison between DCAT and VMAT for liver tumors. *Front Oncol*. (2020) 10:1170. doi: 10.3389/fonc.2020.01170

23. Lee YC, Kim Y. A patient-specific QA comparison between 2D and 3D diode arrays for single-lesion SRS and SBRT treatments. *J Radiosurg SBRT*. (2021) 7:295–307.

24. Bortfeld T, Jiang SB, Rietzel E. Effects of motion on the total dose distribution. *Semin Radiat Oncol*. (2004) 14:41–51. doi: 10.1053/j.semradonc.2003.10.011

25. Netherton T, Li Y, Nitsch P, Shaitelman S, Balter P, Gao S, et al. Interplay effect on a 6-MV flattening-filter-free linear accelerator with high dose rate and fast multi-leaf collimator motion treating breast and lung phantoms. *Med Phys*. (2018) 45:2369–76. doi: 10.1002/mp.12899

26. Burton A, Offer K, Hardcastle N. A robust VMAT delivery solution for single-fraction lung SABR utilizing FFF beams minimizing dosimetric compromise. *J Appl Clin Med Phys*. (2020) 21:299–304. doi: 10.1002/acm2.12919

27. Seco J, Sharp GC, Turcotte J, Gierga D, Bortfeld T, Paganetti H. Effects of organ motion on IMRT treatments with segments of few monitor units. *Med Phys*. (2007) 34:923–34. doi: 10.1118/1.2436972

28. Bezjak A, Paulus R, Gaspar LE, Timmerman RD, Straube WL, Ryan WF, et al. Safety and efficacy of a five-fraction stereotactic body radiotherapy schedule for centrally located non-small-cell lung cancer: NRG oncology/RTOG 0813 trial. *J Clin Oncol*. (2019) 37:1316–25. doi: 10.1200/jco.18.00622

29. Timmerman R, McGarry R, Yiannoutsos C, Papiez L, Tudor K, DeLuca J, et al. Excessive toxicity when treating central tumors in a phase II study of stereotactic body radiation therapy for medically inoperable early-stage lung cancer. *J Clin Oncol*. (2006) 24:4833–9. doi: 10.1200/jco.2006.07.5937

30. Videtic GM, Hu C, Singh AK, Chang JY, Parker W, Olivier KR, et al. A randomized phase 2 study comparing 2 stereotactic body radiation therapy schedules for medically inoperable patients with stage I peripheral non-small cell lung cancer: NRG oncology RTOG 0915 (NCCTG N0927). *Int J Radiat Oncol Biol Phys*. (2015) 93:757–64. doi: 10.1016/j.ijrobp.2015.07.2260

31. Potter NJ, Yan G, Liu H, Alahmad H, Kahler DL, Liu C, et al. Beam flatness modulation for a flattening filter free photon beam utilizing a novel direct leaf trajectory optimization model. *J Appl Clin Med Phys*. (2020) 21:142–52. doi: 10.1002/acm2.12837

32. Shaw E, Kline R, Gillin M, Souhami L, Hirschfeld A, Dinapoli R, et al. Radiation Therapy Oncology Group: radiosurgery quality assurance guidelines. *Int J Radiat Oncol Biol Phys*. (1993) 27:1231–9. doi: 10.1016/0360-3016(93)90548-a

33. Wilke L, Andratschke N, Blanck O, Brunner TB, Combs SE, Grosu A-L, et al. ICRU report 91 on prescribing, recording, and reporting of stereotactic treatments with small photon beams: Statement from the DEGRO/DGMP working group stereotactic radiotherapy and radiosurgery. *Strahlentherapie und Onkologie: Organ der Deutschen Rontgengesellschaft … [et al]*. (2019) 195:193–98. doi: 10.1007/s00066-018-1416-x

34. Craft D, Khan F, Young M, Bortfeld T. The price of target dose uniformity. *Int J Radiat Oncol Biol Phys*. (2016) 96:913–14. doi: 10.1016/j.ijrobp.2016.07.033

35. Xhaferllari I, Chen JZ, MacFarlane M, Yu E, Gaede S. Dosimetric planning study of respiratory-gated volumetric modulated arc therapy for early-stage lung cancer with stereotactic body radiation therapy. *Pract Radiat Oncol*. (2015) 5:156–61. doi: 10.1016/j.prro.2014.08.009

36. Raman S, Yau V, Pineda S, Le LW, Lau A, Bezjak A, et al. Ultracentral tumors treated with stereotactic body radiotherapy: single-institution experience. *Clin Lung Cancer*. (2018) 19:e803–e10. doi: 10.1016/j.cllc.2018.06.001

37. Fernandez DJ, Sick JT, Fontenot JD. Interplay effects in highly modulated stereotactic body radiation therapy lung cases treated with volumetric modulated arc therapy. *J Appl Clin Med Phys*. (2020) 21:58–69. doi: 10.1002/acm2.13028

38. Miften M, Olch A, Mihailidis D, Moran J, Pawlicki T, Molineu A, et al. Tolerance limits and methodologies for IMRT measurement-based verification QA: Recommendations of AAPM Task Group No. *218 Med Phys*. (2018) 45:e53–83. doi: 10.1002/mp.12810

39. Pulliam KB, Huang JY, Howell RM, Followill D, Bosca R, O'Daniel J, et al. Comparison of 2D and 3D gamma analyses. *Med Phys*. (2014) 41:021710. doi: 10.1118/1.4860195

40. Edvardsson A, Nordström F, Ceberg C, Ceberg S. Motion induced interplay effects for VMAT radiotherapy. *Phys Med Biol*. (2018) 63:085012. doi: 10.1088/1361-6560/aab957

41. Seppenwoolde Y, Shirato H, Kitamura K, Shimizu S, van Herk M, Lebesque JV, et al. Precise and real-time measurement of 3D tumor motion in lung due to breathing and heartbeat, measured during radiotherapy. *Int J Radiat Oncol Biol Phys*. (2002) 53:822–34. doi: 10.1016/s0360-3016(02)02803-1

42. Peterlin P, Stanič K, Méndez I, Strojnik A. Treating lung cancer with dynamic conformal arc therapy: a dosimetric study. *Radiat Oncol*. (2017) 12:93. doi: 10.1186/s13014-017-0823-y

43. Yau T, Kempe J, Gaede S. A four-dimensional dynamic conformal arc approach for real-time tumor tracking: A retrospective treatment planning study. *J Appl Clin Med Phys*. (2024) 25:e14224. doi: 10.1002/acm2.14224

44. Mesny E, Ayadi M, Dupuis P, Beldjoudi G, Tanguy R, Martel-Lafay I. Clinical outcomes and lung toxicities after lung SABR using dynamic conformal arc therapy: a single-institution cohort study. *Radiat Oncol*. (2023) 18:36. doi: 10.1186/s13014-023-02227-2

45. Corradetti MN, Haas AR, Rengan R. Central-airway necrosis after stereotactic body-radiation therapy. *N Engl J Med*. (2012) 366:2327–9. doi: 10.1056/NEJMc1203770

46. Nagata Y, Kimura T. Stereotactic body radiotherapy (SBRT) for Stage I lung cancer. *Jpn J Clin Oncol*. (2018) 48:405–09. doi: 10.1093/jjco/hyy034

47. Cuccia F, Mortellaro G, Mazzola R, Donofrio A, Valenti V, Tripoli A, et al. Prognostic value of two geriatric screening tools in a cohort of older patients with early stage Non-Small Cell Lung Cancer treated with hypofractionated stereotactic radiotherapy. *J Geriatr Oncol*. (2020) 11:475–81. doi: 10.1016/j.jgo.2019.05.002

48. Figlia V, Mazzola R, Cuccia F, Alongi F, Mortellaro G, Cespuglio D, et al. Hypofractionated stereotactic radiation therapy for lung Malignancies by means of helical tomotherapy: report of feasibility by a single-center experience. *Radiol Med*. (2018) 123:406–14. doi: 10.1007/s11547-018-0858-7

49. Sande EPS, Acosta Roa AM, Hellebust TP. Dose deviations induced by respiratory motion for radiotherapy of lung tumors: Impact of CT reconstruction, plan complexity, and fraction size. *J Appl Clin Med Phys*. (2020) 21:68–79. doi: 10.1002/acm2.12847

50. Ge C, Wang H, Chen K, Sun W, Li H, Shi Y. Effect of plan complexity on the dosimetry, delivery accuracy, and interplay effect in lung VMAT SBRT with 6 MV FFF beam. *Strahlenther Onkol*. (2022) 198:744–51. doi: 10.1007/s00066-022-01940-3

51. Soda R, Hatanaka S, Hariu M, Shimbo M, Yamano T, Nishimura K, et al. Evaluation of geometrical uncertainties on localized prostate radiotherapy of patients with bilateral metallic hip prostheses using 3D-CRT, IMRT and VMAT: A planning study. *J X-ray Sci technology*. (2020) 28:243–54. doi: 10.3233/xst-190598

52. Duan J, Shen S, Fiveash JB, Popple RA, Brezovich IA. Dosimetric and radiobiological impact of dose fractionation on respiratory motion induced IMRT delivery errors: a volumetric dose measurement study. *Med Phys*. (2006) 33:1380–7. doi: 10.1118/1.2192908

53. Lee S, Lee D, Verma V, Waters D, Oh S, Colonias A, et al. Dosimetric benefits of dynamic conformal arc therapy-combined with active breath-hold in lung stereotactic body radiotherapy. *Med Dosim*. (2022) 47:54–60. doi: 10.1016/j.meddos.2021.08.004

54. Saroj DK, Yadav S, Paliwal N. Does fluence smoothing reduce the complexity of the intensity-modulated radiation therapy treatment plan? A dosimetric analysis. *J Med Phys*. (2022) 47:336–43. doi: 10.4103/jmp.jmp_81_22

55. Gauer T, Sothmann T, Blanck O, Petersen C, Werner R. Under-reported dosimetry errors due to interplay effects during VMAT dose delivery in extreme hypofractionated stereotactic radiotherapy. *Strahlenther Onkol*. (2018) 194:570–79. doi: 10.1007/s00066-018-1264-8

56. Varasteh M, Ali A, Esteve S, Jeevanandam P, Göpfert F, Irvine DM, et al. Patient specific evaluation of breathing motion induced interplay effects. *Phys Med*. (2023) 105:102501. doi: 10.1016/j.ejmp.2022.11.005

57. Vieillevigne L, Bessieres S, Ouali M, Lanaspeze C. Dosimetric comparison of flattened and unflattened beams for stereotactic body radiation therapy: Impact of the size of the PTV on dynamic conformal arc and volumetric modulated arc therapy. *Phys Med*. (2016) 32:1405–14. doi: 10.1016/j.ejmp.2016.10.007

58. Bokrantz R, Wedenberg M, Sandwall P. Dynamic conformal arcs for lung stereotactic body radiation therapy: A comparison with volumetric-modulated arc therapy. *J Appl Clin Med Phys*. (2020) 21:103–09. doi: 10.1002/acm2.12800